MOLECULAR AND CELLULAR BIOLOGY, July 2008, p. 4261–4274 Vol. 28, No. 13
0270-7306/08/$08.00+0 doi:10.1128/MCB.02252-07

GTPase-Mediated Regulation of the Unfolded Protein Response in *Caenorhabditis elegans* Is Dependent on the AAA$^+$ ATPase CDC-48▽†

Marie-Elaine Caruso,[1] Sarah Jenna,[1]‡ Marion Bouchecareilh,[2] David L. Baillie,[3] Daniel Boismenu,[4] Dalia Halawani,[5] Martin Latterich,[5] and Eric Chevet[1,2,6]*

Department of Surgery, McGill University, Montreal, QC, Canada[1]; INSERM, U889, Team Avenir, Bordeaux, France[2]; Department of Molecular Biology and Biochemistry, Simon Fraser University, Burnaby, BC, Canada[3]; McGill University and Génome Quebec Innovation Centre, Montreal, QC, Canada[4]; Faculty of Pharmacy, University of Montreal, Montreal, QC, Canada[5]; and University Bordeaux 2, Bordeaux, France[6]

Received 20 December 2007/Returned for modification 7 January 2008/Accepted 10 April 2008

When endoplasmic reticulum (ER) homeostasis is perturbed, an adaptive mechanism is triggered and named the unfolded protein response (UPR). Thus far, three known UPR signaling branches (IRE-1, PERK, and ATF-6) mediate the reestablishment of ER functions but can also lead to apoptosis if ER stress is not alleviated. However, the understanding of the molecular mechanisms integrating the UPR to other ER functions, such as membrane traffic or endomembrane signaling, remains incomplete. We consequently sought to identify new regulators of UPR-dependent transcriptional mechanisms and focused on a family of proteins known to mediate, among other, ER-related functions: the small GTP-binding proteins of the RAS superfamily. To this end, we used transgenic UPR reporter *Caenorhabditis elegans* strains as a model to specifically silence small-GTPase expression. We show that the Rho subfamily member CRP-1 is an essential component of UPR-induced transcriptional events through its physical and genetic interactions with the AAA$^+$ ATPase CDC-48. In addition, we describe a novel signaling module involving CRP-1 and CDC-48 which may directly link the UPR to DNA remodeling and transcription control.

The endoplasmic reticulum (ER) is an organelle found in eukaryotic cells, which is mainly involved in calcium sequestration, lipid biosynthesis and translation, folding, and transport of secretory proteins (9). These functions require specialized and integrated molecular machines (7). Most of the proteins distributed in organelles of the secretory pathway, expressed at the cell surface or secreted, transit through the ER before reaching their final destination. Indeed, polypeptide chains, translated on ER membrane-bound ribosomes, are first translocated into the ER lumen via the translocon and then processed through the ER folding machineries, which include a chaperone component (e.g., BiP or GRP94), a posttranslational modification machinery (e.g., N glycosylation with the oligosaccharyl transferase complex, S-S bound formation with the protein disulfide isomerases), and a quality control component (e.g., calnexin, UDP-glucose:glycoprotein glucosyltransferase). Proteins which do not acquire a correct conformation are retained in the ER by ER-specific quality control mechanisms and are consequently granted further folding attempts. If this fails again, terminally misfolded proteins are degraded via the ER-associated degradation (ERAD) machinery (9).

Under basal conditions, these integrated mechanisms maintain the ER protein load in equilibrium with ER's folding and export capacities. However, if one of those components is dysfunctional, the entire chain reaction is perturbed and ER homeostasis is disrupted. This leads to an increased amount of improperly folded proteins, which accumulate within the ER. As a mechanism for adaption to this phenomenon, cells have evolved the unfolded protein response (UPR), which aims at restoring ER homeostasis (38, 41) by (i) attenuating protein translation, (ii) increasing ER folding capacity, (iii) increasing ERAD capacity, and (iv) triggering cell death if ER homeostasis is not restored. This stress response is regulated by the activation of three ER resident proximal sensors, which constitute the three arms of the UPR: inositol-requiring enzyme 1 (IRE-1), activating transcription factor 6 (ATF-6), and protein kinase RNA-like ER kinase (PERK) (38, 41).

Another mechanism regulating ER content is mediated by the export machinery. For instance, activation of the UPR was shown to induce the expression of the small G protein SAR-1, a member of the COPII protein complex (28, 40, 43). Moreover, expression of a dominant negative SAR-1 induces the accumulation of proteins in the ER (28, 40, 43), probably leading to the saturation of ER folding capacity. In addition to the role of SAR-1 in the regulation of ER protein load, other GTPases of the RAS superfamily were found to play a role in either organelle maintenance/biogenesis (2, 24) or endomembrane signaling (33–35).

These observations led us to postulate that small GTP binding proteins of the RAS superfamily may represent a master regulatory component of ER homeostasis. To test this hypothesis, we investigated the involvement of these GTPases in the activation of the UPR using RNA interference (RNAi) in *Caenorhabditis elegans*. This experimental system constitutes a

* Corresponding author. Mailing address: Team Avenir, INSERM U889, Université Bordeaux 2, 146 rue Léo Saignat, 33076 Bordeaux, France. Phone: 33 (0)5 57 57 92 53. Fax: 33 (0)5 56 51 40 77. E-mail: eric.chevet@u-bordeaux2.fr.

† Supplemental material for this article may be found at http://mcb.asm.org/.

‡ Present address: Dept. of Chemistry, UQAM, Montreal, QC, Canada.

▽ Published ahead of print on 5 May 2008.

powerful model in which the three UPR arms are conserved and which contains over 60 conserved GTPases of the RAS superfamily. Based on the analysis of a GTPase family subset, our results indicate the specific roles of members of the Rho family of GTPases in the transcriptional activation of UPR target genes. We found that this is possibly regulated through the presence of CRP-1 in a complex with the AAA^+ ATPase CDC-48. We demonstrate physical and genetic interactions between CRP-1 and CDC-48 and consequently delineate a novel signaling component physically linking ER stress and transcriptional regulation in metazoans.

MATERIALS AND METHODS

***C. elegans* strains.** The wild-type strain N2 (Bristol) was used as the reference strain. Knockout mutant alleles *ok685* (*crp-1*$^{-/-}$; Y32F6B.3), *gk186* (*atm-1*$^{-/-}$; Y48G1BL.2), *tm544* (*cdc-48.1*$^{-/-}$; C06A1.1), *ok275* (*pek-1*$^{-/-}$; F46C3.1), and *ok551* (*atf-6*$^{-/-}$; F45E6.2) were obtained from the *Caenorhabditis* Genetics Center at the University of Minnesota. *promoter*::*gfp* reporter strains BC10700 (ZK632.6), BC13719 (F48E3.3), BC11945 (F43E2.8), BC10066 (C15H9.6), BC13607 (B0403.4), BC10371 (C53B4.7A), BC14636 (B0285.9), and BC10178 (C55B6.2) were obtained from the British Columbia *C. elegans* Gene Expression Consortium. *C. elegans* animals were maintained at 20°C under standard culture conditions and fed with OP50 unless otherwise mentioned (5).

Drug induction and GFP quantification. ER stress level was measured using transgenic worms expressing green fluorescent protein (GFP) under the control of various ER stress promoters. Synchronized L1 populations expressing the different ER stress GFP reporters were grown on standard nematode growth medium (NGM) plates. L4 stage worms were then transferred on NGM plates containing dimethyl sulfoxide as control, 5 μg/ml tunicamycin (TM), 5 mM L-azetidine-2-carboxylic acid (AZC), 1 mM dithiothreitol (DTT), or 1 μM thapsigargin (TG) for 5 h at 20°C. Fluorescence quantification was performed using two different methods. Entire worm populations were analyzed using the Copas Biosort (Union Biometrica) (11), which provided an average fluorescence level for the entire worm population ($n \geq 1{,}000$). These results were correlated with an observation-based counting method using fluorescence microscopy in which worms were classified in three groups of (i) low, (ii) medium, and (iii) high levels of fluorescence. At least 100 worms were counted per strain and condition in triplicate by at least two independent investigators. Moreover, to validate the counting methodology, a blinded evaluation of fluorescence was correlated with an immunoblot using anti-GFP antibodies on worm lysates. As expected, the highest signal observed by immunoblotting correlated with the highly fluorescent worm population.

Tissue localization. Expression profiles were analyzed using GFP-reporter transgenic worms (19). Following a 5-h treatment with 5 μg/ml TM at 20°C, living worms were mounted on agarose pads in M9 buffer containing 1 mM levamisole (Sigma). Fluorescence emission from living worms was observed using an Axiovert-200 microscope (Zeiss), and images were analyzed using Northern Eclipse, version 6.0 (Empix Imaging, Mississauga, Ontario, Canada).

RNAi. All RNAi experiments were carried out using a feeding procedure described previously (21). RNAi constructs were either cloned from a *C. elegans* cDNA library (de novo) or retrieved from the *C. elegans* ORFeome collection, version 1.1 (37), using the Gateway technology (Invitrogen). For primers used for de novo cloning, see Table S1 in the supplemental material. GTPase open reading frames (ORFs), without ATG, and approximately 500 base pairs of the *cdc-48.1* (C06A1.1) and *xbp-1* (R74.3) genes were amplified by PCR using Platinum *Taq* high-fidelity DNA polymerase (Invitrogen) and the following amplification scheme: denaturation at 94°C for 40 s, annealing at 60°C for 40 s, and elongation at 72°C for 1 min for 35 cycles. These PCR products were polyethylene glycol precipitated and recombined into pDONR201 using the Gateway BP Clonase (Invitrogen). These entry clones were subsequently recombined, using LR Clonase, into Gateway-compatible pL4440 vector and transformed into HT115(DE3) bacteria. Isolated transformant bacteria were grown for 12 h at 37°C in Luria-Bertani medium supplemented by 100 μg/ml ampicillin. Bacteria were spotted on NGM plates containing 1 mM IPTG (isopropyl-β-D-thiogalactopyranoside) and 100 μg/ml ampicillin, dried, and induced overnight at room temperature. Synchronized L1 worm populations were transferred to these plates and treated for three days. L4 worms were then transferred to new RNAi plates containing or not 5 μg/ml TM, and fluorescence levels were analyzed as described above, following 5 hours of incubation at 20°C.

ORF cloning, expression, and pull-down affinity purification. Recombinant *C. elegans* GST–CRP-1 and GST–CDC-42 and mouse His_6–p97/VCP/CDC-48 (which displays 76% identity with CeCDC-48) proteins were expressed in *Escherichia coli* as previously described (8, 23) and purified using glutathione-Sepharose 4B or nickel-nitrilotriacetic acid (NTA)-agarose, respectively. The ORFs encoding CDC-48.1, CDC648.2, and HIM-6 were amplified by reverse transcription-PCR (RT-PCR) using the indicated primers (see Table S1 in the supplemental material) from *C. elegans* total RNA. The amplified PCR products were cloned by recombination into the pDONR201 vector using the Gateway technology (Invitrogen). The entry vectors generated were then used to recombine the specific ORFs into His_6-Nterm or Strep tag-Nterm prokaryotic expression vectors. These were then transformed into DH5a bacteria. Five individual colonies were picked and pooled, and plasmid DNA was amplified and transformed into BL21 cells. Recombinant proteins were produced in BL21 cells following a 3-h induction using either 1 mM IPTG or 0.2 μg/ml tetracycline. Protein lysates were either directly frozen or directly subjected to affinity purification as recommended by the manufacturers. For one set of experiments (see Fig. 4), we used bacterial lysate expressing recombinant proteins. In these conditions, GST–CRP-1 or GST–CDC-42 (in equal amounts) was mixed with mouse His_6–p97/VCP/CDC-48-expressing bacterial lysate and the mixture was incubated for 2 hours at 4°C. GST pull-down was then carried out on bacterial lysate using glutathione-Sepharose 4B resin (GE Biosciences). Following incubation for an additional hour at 4°C, beads were washed six times with phosphate-buffered saline and resolved by sodium dodecyl sulfate-polyacrylamide gel electrophoresis (SDS-PAGE). Proteins were revealed using Coomassie blue R250 staining. His_6 pull-down was carried out on N2 or *crp-1*$^{-/-}$ (*ok685*) allele strains mixed with purified His_6–p97/VCP/CDC-48 proteins for 2 hours at 4°C. Complexes were purified using Ni-NTA-agarose (Qiagen) and resolved by SDS-PAGE. Gels were then transferred on nitrocellulose membranes and subjected to standard immunoblot protocols using either mouse anti-p97/VCP/CDC-48 (Abnova) or hen anti-CRP-1 antibodies (HyperOmics Farma, Inc., Montreal, QC, Canada). For the other set of experiments (see Fig. 5), purified proteins (1 μg) were incubated with 10 mM Tris, pH 7.4, and 100 mM NaCl (in the presence or not of 10 μM GTP and ATP) for 2 h at 4°C and pulled down with beads for 45 min under rotation at 4°C. Following five washes using the same buffer as above but containing 0.5% Triton X-100, the beads were resuspended in 2× Laemmli sample buffer, resolved by electrophoresis, and immunoblotted using anti-glutathione *S*-transferase (GST; Cellular Signaling) or anti-Strep tag (Qiagen) antibodies.

CRP-1 pull-down analyses. Worm protein extracts were prepared as previously described (19). Briefly, worms were washed five times using M9 medium to remove bacteria and suspended in homogenization buffer (15 mM HEPES, pH 7.6, 10 mM KCl, 0.1 mM EDTA, 0.5 mM EGTA, 44 mM sucrose, 1 mM DTT, protease inhibitor cocktail [Roche]) and sonicated, and the resulting lysate was cleared by centrifugation at 13,500 rpm for 15 min at 4°C. GST pull-down assays were performed on total worm lysate precleared with glutathione-Sepharose beads bound to GST or Ni-NTA beads to remove all nonspecific binding. Precleared lysates were then mixed with purified GSP–CRP-1 on glutathione-Sepharose 4B or His_6–p97/VCP/CDC-48 on Ni-NTA beads and incubated for 2 h at 4°C. After five washes, beads were suspended using 2× Laemmli buffer and proteins were resolved by SDS-PAGE. The resulting gel was stained using Coomassie blue R250 and processed for mass spectrometry (see methods in the supplemental material).

Data analyses. The human ortholog of each hit identified in the CRP-1 pull-down was retrieved from NCBI, ENSEMBL, or other large sequence repositories when existing or available. The corresponding list was then analyzed using the STRING suite (46, 47) to evaluate the potentially existing functional interactions between proteins found in the CRP-1 complex. We also added a subnetwork including the first-degree genetic or physical interactor of His_6–p97/VCP/CDC-48. The resulting scale-free functional interaction network was then annotated using the Medusa program (16).

TM sensitivity assay. N2 worms and mutant strains were treated using the alkaline hypochlorite method (0.5 M NaOH, H_2O, and 0.8% bleach) to isolate embryos. Eggs were hatched overnight in M9 medium (40 mM Na_2HPO_4, 20 mM KH_2PO_4, 8 mM NaCl, 20 mM NH_4Cl) to obtain an L1-synchronized population. L1 worms were transferred onto NGM plates containing various concentrations of TM (0, 2, 5, or 10 μg/ml) and seeded on HT115 cells expressing or not double-stranded RNA (dsRNA) for the target genes (see "RNAi" for conditions). The developmental stage was analyzed after 24 and 48 h at 20°C, and the percentages of L1 larvae and dead worms over the total population were determined and reported.

RT-PCR analyses. Worms (N2 or *crp-1*$^{-/-}$) were treated or not with 5 μg/ml TM and 2 mM DTT for 5 h or 10 mM NaN_3 for 90 min. They were then collected and lysed using Trizol (Invitrogen). Total RNA was then extracted as recom-

A

Gene name	Sequence name	GFP-reporter strains	Human orthologs	NCBI protein ID	e value	References
hsp-4	F43E2.8	BC11945	HSPA5 (BiP)	NP_005338.1	4.10E-269	Urano, 2002 Shen, 2001
ckb-2	B0285.9	BC14636	Choline/ethanolamine kinase	NP_005189.2	1.50E-28	Urano, 2002
hsp-3	C15H9.6	BC10066	HSPA5 (BiP)	NP_005338.1	4.20E-276	Urano, 2002 Shen, 2001
tag-320	B0403.4	BC13607	protein disulfide isomerase A6	NP_005733.1	3.90E-132	Urano, 2002
cnx-1	ZK632.6	BC10700	calnexin precursor	NP_001737.1	5.79E-127	
dnj-7	C55B6.2	BC10178	DnaJ	NP_006251.1	3.60E-114	Urano, 2002
	F48E3.3	BC13719	UDP-glucose:glycoprotein glucosyltransferase 2	NP_064506.2	3.90E-290	
bre-1	C53B4.7	BC10371	GDP-mannose 4,6 dehydratase	NP_001491.1	1.10E-128	Urano, 2002

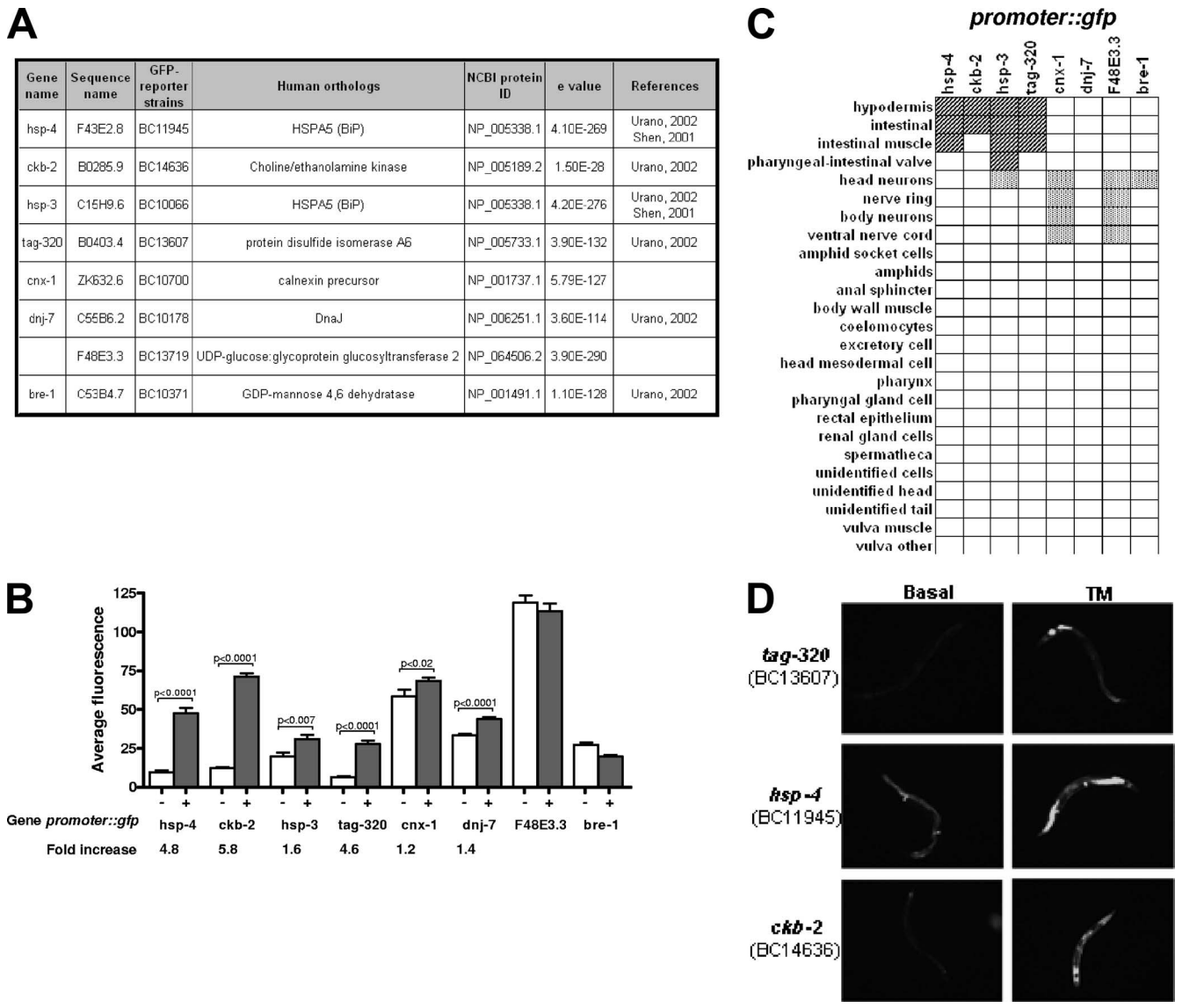

FIG. 1. Identification and characterization of powerful ER stress GFP reporter genes. (A) List of ER stress *promoter::gfp* reporter genes successfully constructed, with the strain name and the human ortholog information. (B) Fluorescence induction of the eight GFP reporter genes when treated with 5 μg/ml TM. Fluorescence level was quantified on entire transgenic worm populations (≥1,000 worms per conditions) using the Copas Biosort. The increase is the ratio between the average fluorescence under TM conditions compared to the basal fluorescence level of each strain. (C) Expression pattern of each GFP reporter strain in living animals. Intestine expression and neuronal expression are represented in light gray and dark gray, respectively. (D) Fluorescence microscopy pictures for the three strains with the highest increases in fluorescence (*tag-320*, *hsp-4*, and *ckb-2* strains) under basal conditions or after TM treatment.

mended by the manufacturer and reverse transcribed using the Superscript III kit (Invitrogen). PCR products were then amplified using the primers described in Table S1 in the supplemental material within the linear part of the amplification curve, resolved on agarose gels, and visualized following ethidium bromide staining. Transcript expression was normalized to that of *ama-1*.

RESULTS

ER stress-mediated activation of *hsp-4*, *ckb-2*, and *tag-320* promoters in *C. elegans* intestine. To study the implication of small G proteins of the RAS superfamily in the maintenance of ER homeostasis, we developed an experimental system allowing efficient and rapid ER stress detection. To this end, we used a *Caenorhabditis elegans*-based GFP reporter driven by UPR-responsive promoters. We selected these promoters based upon their previously reported activation upon ER stress using, for instance, microarray studies (6, 45). Practically, a putative promoter region of 2.5 kilobases cloned upstream of each target gene was fused to the GFP gene (*gfp*) cDNA. These constructs were used to generate transgenic worm lines expressing GFP under the control of putative UPR-induced promoters (11, 17, 27). The strains successfully created are listed in Fig. 1A. Also listed in this figure are the gene and sequence names as they appear in WormBase (http://www.wormbase.org/), as well as the names of the corresponding human orthologs. *hsp-4* and *hsp-3* are the two *C. elegans* homologs of the

mammalian ER chaperone GRP78/BiP gene. Expression of the GFP reporter under the control of endogenous promoters from both genes was previously shown to increase upon TM treatment (22), and these results were confirmed using our BC11945 (*phsp-4*::*gfp*) and BC10066 (*phsp-3*::*gfp*) strains (Fig. 1B). The six other GFP reporters used in our study expressed GFP under the control of various promoters: the ER protein disulfide isomerase-like protein-encoding gene (*ptag-320*::*gfp*), the heat shock protein p58 (DnaJ)-encoding gene (*pdnj-7*::*gfp*), the choline/ethanolamine kinase-encoding gene (*pckb-2*::*gfp*), and three genes involved in ER quality control, the calnexin (*pcnx-1*::*gfp*), UDP-glucose:glycoprotein glucosyltransferase 2 (*pF48E3.3*::*gfp*), and GDP-mannose-4,6-dehydratase (*pbre-1*::*gfp*) genes (Fig. 1A). To test whether these transgenic lines were able to activate the selected GFP reporters upon ER stress, we treated adult hermaphrodites with TM, an antibiotic that inhibits N glycosylation (15) and strongly induces the UPR. We measured and quantified GFP expression level using the Copas Biosort (Union Biometrica) (11, 20). This instrument is designed to perform multiparametric analyses of micrometric particles in a semiautomated manner. This allowed us to measure the average fluorescence emitted by a large population of transgenic worms (1,000 animals per conditions) in response to TM treatment. Fluorescence levels of *phsp-4*::*gfp* (BC11945), *pckb-2*::*gfp* (BC14636), *phsp-3*::*gfp* (BC10066), *ptag-320*::*gfp* (BC13607), *pcnx-1*::*gfp* (BC10700), and *pdnj-1*::*gfp* (BC10178) strains were significantly increased upon TM treatment, whereas those of the *pF48E3.3*::*gfp* (BC13719) and *pbre-1*::*gfp* (BC10371) strains were not (Fig. 1B).

To select the most appropriate GFP reporter strains for our study, we also analyzed, using fluorescence microscopy, GFP tissue expression profiles of the strains described above. Interestingly, *phsp-4*::*gfp*, *pckb-2*::*gfp*, *phsp-3*::*gfp*, and *ptag-320*::*gfp* reporters, shown to have the highest GFP expression, increased upon TM treatment 4.8-, 5.8-, 1.6-, and 4.6-fold, respectively, were expressed mainly in the intestine (Fig. 1C and D). In contrast, reporters such as *pcnx-1*::*gfp*, *pF48E3.3*::*gfp*, and *pbre-1*::*gfp*, which were less sensitive to TM, were principally expressed in the nervous system (Fig. 1C). Differences in GFP expression upon TM treatment may result from a greater sensitivity/accessibility of certain organs/cell types (for example, the intestine) and also the relative sizes of the organs. We therefore concluded that *phsp-4*::*gfp*, *pckb-2*::*gfp*, and *ptag-320*::*gfp* were the three most efficient reporters to detect and measure the ER stress-mediated transcriptional response.

ER stress-responsive promoters are specifically activated upon treatment with different ER stress inducers. To determine if the induction of fluorescence observed in the three most responsive GFP-reporter strains was TM specific, we treated transgenic animals using various chemicals known to induce ER stress in cultured mammalian cells. Worms were exposed to four different agents, including TM, that act differentially on the ER but ultimately lead to ER stress. AZC is a proline analogue which causes defects in protein conformation when integrated into the polypeptide chain (10). DTT is a reducing agent that affects the ER lumen oxidative environment (4), and, finally, TG is a Ca^{2+}-ATPase (SERCA) inhibitor that causes ER Ca^{2+} depletion (39). As shown in Fig. 2, the three GFP reporter strains tested responded differentially to the four ER stress inducers selected. In our experimental setup, TM was the strongest ER stress inducer for the *pckb-2*::*gfp*, *phsp-4*::*gfp*, and *ptag-320*::*gfp* strains with, respectively, 78%, 80%, and 22% of the worm population expressing a high level of fluorescence following a 5-hour treatment. AZC and DTT had mainly the same impact on the three reporters, with almost 49% of worms expressing high fluorescence in the *pckb-2*::*gfp* strain, 28% in the *phsp-4*::*gfp* strain, and less than 20% in the *ptag-320*::*gfp* strain. Finally, TG had a higher level of fluorescence induction in the *pckb-2*::*gfp* strain, with 61% of the worm population expressing high fluorescence. These results show that *pckb-2*::*gfp* is the reporter which presents the highest and most homogenous response to diverse ER stress treatments. In addition, they indicate that, in our experimental settings, TM represents the most universal ER stress inducer. For these reasons, we selected the *pckb-2*::*gfp* reporter to identify, using RNAi, new ER signaling regulators and TM to induce ER stress in *C. elegans*.

CRP-1 expression is necessary for a TM-induced ER stress transcriptional response. In an attempt to identify small GTP-binding proteins involved in ER stress signaling events, we subjected the *pckb-2*::*gfp* reporter strain to RNAi treatments targeting specific GTPases (Table 1). Variations were measured using fluorescence microscopy, under basal conditions or following a 5-hour treatment with TM. Three controls were used to evaluate RNAi efficiency and specificity. *pckb-2*::*gfp* reporter worms were treated with an empty RNAi vector, an RNAi vector against GFP, or RNAi vectors containing GTPase coding sequences but for which production of dsRNA was not induced by IPTG (see Materials and Methods). These controls supported the validity and efficacy of our experimental system.

Based on the current knowledge on small GTPases of the RAS superfamily in *C. elegans*, we focused on 13 *C. elegans* GTPases whose mammalian orthologs were either localized in the ER or along the secretory pathway and/or known to regulate ER-related functions (Table 1). RNAi treatment targeting these GTPases revealed that they could be divided into four different categories according to their effect on the activation of the *ckb-2* promoter under basal conditions or upon TM exposure (Table 1). The first category contained most of the GTPases tested (8/13), which did not have any effect on *pckb-2*::*gfp* activation. The second category contained GTPases for which RNAi-mediated silencing led to a severe phenotype such as L1 arrest of lethality and for which GFP expression could not be measured in adult worms. Two GTPases, RAB-1 and RAB-7, were found to be in this category and were excluded from further analysis (Table 1).

The two other categories included GTPases for which alteration of expression levels had significant effects on ER stress-mediated *pckb-2*::*gfp* activation under basal conditions or following treatment. Representative results obtained for these GTPases are shown in Fig. 3A. In the third category, we identified one GTPase, SAR-1, whose silencing led to an activation of *pckb-2*::*gfp* under basal conditions. This is consistent with the previous observations that SAR-1 was implicated in membrane transport from the ER to the Golgi apparatus (43). In addition, our results suggest that disruption of this transport would inhibit protein progression from the ER (43) and consequently induce the UPR. The fourth category contains two GTPases, CDC-42 and CRP-1, whose silencing prevented

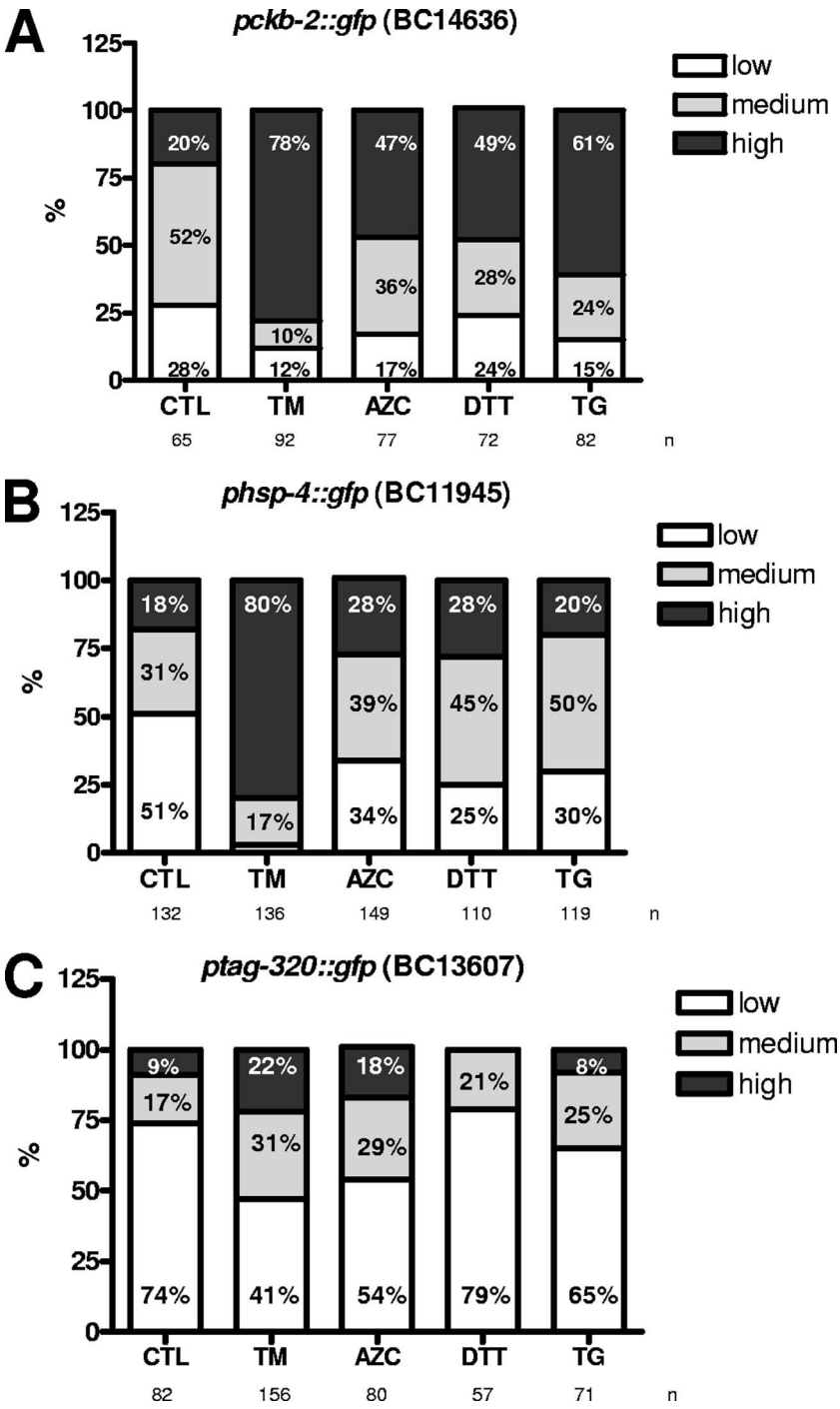

FIG. 2. ER stressors TM, AZC, DTT, and TG act differentially on the three most responsive GFP reporter strains. Populations of (A) *pckb-2*::*gfp* (BC14636), (B) *phsp-4*::*gfp* (BC11945), and (C) *ptag-320*::*gfp* (BC13607) strains were treated with 5 μg/ml TM, 10 μM AZC, 2 mM DTT, and 5 μM TG for 5 hours and visualized and quantified using a fluorescence microscope. The percentage of worms with a low, medium, or high level of fluorescence was plotted against the different chemicals. Experiments were performed at least twice in duplicate. CTL, control.

pckb-2::*gfp* activation after TM exposure. CDC-42 is a small GTPase that regulates actin dynamics and has also been involved in Golgi-to-ER vesicle trafficking events in mammalian cells (25). CRP-1 is a small G protein which clustered with the Rho subfamily according to its amino acid sequence and showed 45% identity to CDC-42 (19) (Table 1). We previously showed that CRP-1 is implicated in the regulation of membrane trafficking in intestinal cells (19) and that CRP-1 RNAi specifically targets CRP-1 expression (see Fig. S1 in the supplemental material). Quantification of total fluorescence of a worm population clearly showed that *crp-1* silencing significantly led to a reduced activation of the *pckb-2*::*gfp* reporter

TABLE 1. Characteristics of the GTPases selected for the first screen and their effect on *pckb-2*::*gfp* reporter activation[a]

Phenotype	WormBase ID[b]	Designation	Subcellular localization[c]	Functions related to the ER (reference)
No effect	C44C11.1	RAS-1	Endomembrane (ER/G)	Intracellular protein transport, ER signal transduction (33)
	F53G12.1	RAB-11.1	TGN recycling/exocytic compartment	Membrane fusion, vesicular trafficking
	F54C9.10	ARL-1	TGN/G	Membrane fusion and traffic
	F53F10.4	UNC-108	ER/*cis*-G	Endocytosis, membrane fusion, vesicular trafficking
	W01H2.3	RAB-37	Secretory granules	Vesicle exocytosis
	ZK792.6	LET-60	Endomembrane (ER/G)	Intracellular protein transport, ER signal transduction (33)
	C27B7.8	RAP-1	G	Membrane fusion, vesicular trafficking
	F45E4.1	ARF-1.1	G/ERGIC/TGN	Mitotic Golgi fragmentation, vesicular trafficking
Severe developmental defects	C39F7.4	RAB-1	ER/*cis*-G	Intracellular vesicle trafficking
	W03C9.3	RAB-7	ER/LE/endosome	Endosomal traffic, vesicular trafficking
Induction of basal ER stress	ZK180.4	SAR-1	ER	ER-to-Golgi protein transport
ER stress inhibition	R07G3.1	CDC-42	ER/G	Cell polarity, protein trafficking
	Y32F6B.3	CRP-1	TGN/RE	Membrane trafficking, cell polarity (19)

[a] *pckb-2*::*gfp* reporter worms were treated with selected GTPase RNAi vectors and exposed or not to TM for 5 hours. The consequence of GTPase silencing on the activation of *ckb*-2 promoters was measured using a fluorescence microscope, and GTPases were classified according to their effect on this reporter into four categories.
[b] ID, identification.
[c] G, Golgi apparatus; TGN, *trans*-Golgi network; ERGIC, ER-Golgi intermediate compartment; LE, late endosomes; RE, recycling endosomes.

under ER stress conditions (Fig. 3B). Our results suggest that both CRP-1 and CDC-42 may be specifically involved in the transmission/establishment of ER stress signals in *C. elegans*.

CRP-1 interacts with CDC-48. To investigate the mechanisms by which CRP-1 may contribute to *pckb-2*::*gfp* induction upon TM treatment, we sought to characterize CRP-1 molecular partners. To this end, we performed a CRP-1 GST pull-down on *C. elegans* total protein extracts followed by SDS-PAGE and mass spectrometry analysis. We identified 20 proteins with various functions, out of which one, the ATPase CDC-48.1 (C06A1.1), which is orthologous to the transitional ER AAA^+ ATPase P97/VCP/CDC-48, was previously reported to display ER-related specific functions (Fig. 4A; see Table S2 in the supplemental material). In addition, although a Mascot search indicated that the hit corresponded to CDC-48.1, the peptides identified by de novo sequencing were common to both CDC-48.1 and CDC-48.2.

CDC-48 has been implicated in the ERAD pathway and in ER membrane fusion (13) and has been identified as a regulator of the ER stress response (48). We confirmed the interaction between CRP-1 and CDC-48 using both GST–CRP-1 and the mouse His_6–P97/VCP/CDC-48 fusion protein expressed in *E. coli*. In this experiment, *E. coli* lysates containing either GST–CRP-1 or GST–CDC-42 were mixed with His_6–P97/VCP/CDC-48-containing lysate followed by pull-down using glutathione-Sepharose beads. As shown in Fig. 4B, P97/VCP/CDC-48 was found in the CRP-1 complex, thus confirming the mass spectrometry analyses. Interestingly, no interaction between P97/VCP/CDC-48 and CDC-42 was detected under these conditions (Fig. 4B). The reverse experiment was also carried out using N2 and CRP-$1^{-/-}$ (allele *ok685*) (19) worm lysates, which were pulled-down using His_6-P97/VCP/CDC48 immobilized on Ni-agarose beads (Fig. 4B). As expected, a complex between P97/VCP/CDC-48 and CRP-1 was observed in wild-type animals but not in the CPR-$1^{-/-}$ worm lysates. The hypothesis supporting a functional interaction between CRP-1 and CDC-48 was also reinforced using *cdc-48.1* silencing in *pckb-2*::*gfp* reporter worms. As observed for *crp-1*, reduction of *cdc-48.1* expression led to an inhibition of TM-induced *pckb-2*::*gfp* reporter activation (Fig. 4C). This phenotype suggests that *pckb-2*::*gfp* activation by TM requires both CRP-1 and CDC-48.1.

Among the proteins identified by mass spectrometry, two other hits presented some interest. Indeed, ATM-1 (Y48G1BL.2) and HIM-6 (T04A11.6) are, respectively, an ortholog of the human protein kinase ATM and the human Bloom syndrome helicase (BLM), a RecQ-like ATP-dependent DNA helicase. BLM was shown to be a direct substrate of ATM, and both proteins are required for optimal repair during DNA replication (1, 36). Recently, p97/VCP/CDC-48 was also shown to be a direct substrate of ATM kinase, but the physiological function of this interaction remains unclear (26). Finally, it was shown that p97/VCP/CDC-48 interacted with another RecQ helicase, WRN, and modulated its localization and functions (18). As a consequence, we postulated that we might have purified a complex of proteins implicated in DNA repair, DNA remodeling, or transcriptional processes and containing at least CRP-1, CDC-48, and ATM-1.

Using the STRING program suite (http://string.embl.de/), a database for the retrieval of known and predicted gene/proteins interactions (46, 47), we built a network based on the human orthologs of the *C. elegans* proteins identified in the CRP-1 GST pull-down (Fig. 4D, white nodes; see Table S3 in the supplemental material). Interestingly, 9 out of the 20 proteins identified by mass spectrometry (Fig. 4D, white nodes) were found to belong to a specific subnetwork implicated in DNA processes (Fig. 4D, black nodes) and including the transcriptional activator p53, ATM, BLM, and P97/VCP/CDC-48. In contrast, none of the proteins found in complex with CRP-1 belonged to the other p97/VCP/CDC-48 subnetwork functionally related to ERAD or membrane fusion (Fig. 4D, gray nodes). In addition, when we attempted to identify other po-

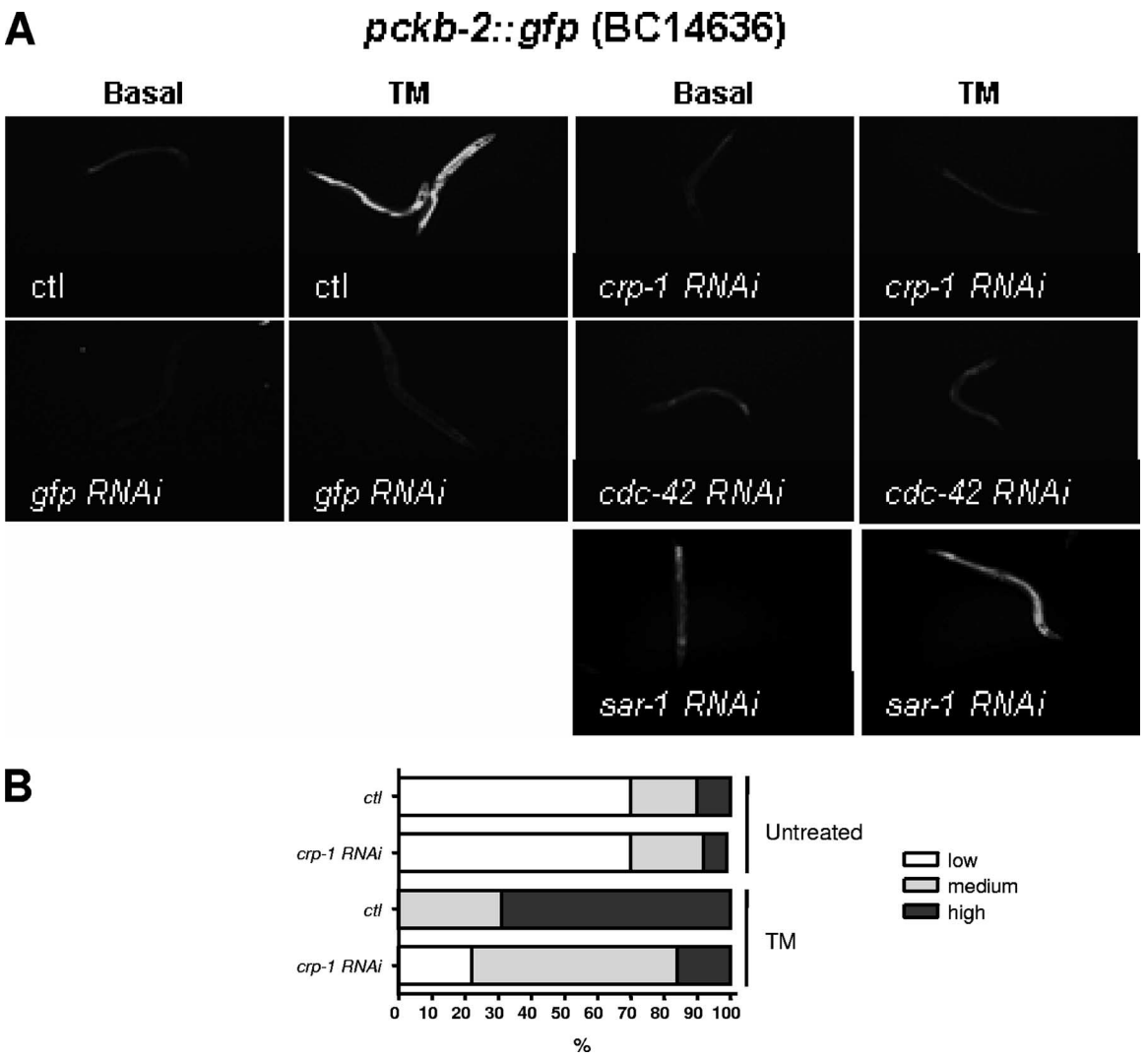

FIG. 3. Effect of *crp-1*, *cdc-42*, and *sar-1* silencing on *ckb-2* promoter activation upon ER stress. (A) Qualitative microscopic pictures for two controls (no RNAi induction [ctl] or GFP RNAi) and three GTPases that gave the most significant results for *pckb-2*::*gfp* reporter activation (encoded by *crp-1*, *cdc-42*, and *sar-1*). (B) Quantification of fluorescence induction of *pckb-2*::*gfp* subjected or not to *crp-1* RNAi and exposed or not to 5 μg/ml TM.

tential functional networks in which proteins found in the CRP-1 GST pull-down could be enriched, no significant other group could be generated (data not shown). This specific functional enrichment further supported the idea that CRP-1 might interact with a protein complex implicated in DNA remodeling/transcription.

Physical interactions regulating the complex including CRP-1, CDC-48, and HIM-6. To further evaluate the relevance of a protein complex including CRP-1, HIM-6, and CDC-48, we evaluated the in vitro interactions between these three proteins. To this end, we used the previously described GST–CRP-1 as well as bacterial recombinant HIM-6 and CDC-48.1, both N-terminally tagged by either six histidine residues or a Strep tag and produced as described in Materials and Methods. We established the existence of six possible interactions to be tested in vitro. We first tested the direct interactions between CRP-1 and HIM-6 and between CRP-1 and CDC-48.1. As shown in Fig. 5A, CRP-1 did not directly bind to HIM-6 but, as expected from the results obtained in Fig. 4, directly interacted with CDC-48.1 (similar results were obtained with CDC-48.2 [data not shown]). We then evaluated the association between HIM-6 and CDC-48.1. To this end, six-His-tagged CDC-48.1 or HIM-6 was incubated in the presence of Strep-tagged HIM-6 or CDC-48.1, respectively; the mixture was then pulled-down using Ni-NTA-agarose beads and immunoblotted using anti-Strep tag antibodies. These experiments revealed that HIM-6 directly associated with CDC-48.1 (Fig. 5B). This result was not that surprising, as P97, the mammalian ortholog of CDC-48, binds to the Werner syndrome RecQ helicase, which is homologous to BLM, the mammalian ortholog of HIM-6. In an attempt to test for the existence of a ternary complex, we incubated GST–CRP-1 with Strep-tagged HIM-6 and increasing concentrations of His_6–CDC-48.1 (Fig. 5C). The mixture was then subjected to a pull-down using glutathione-Sepharose beads and immunoblotted using anti-Strep tag antibodies. The analysis revealed the existence of a

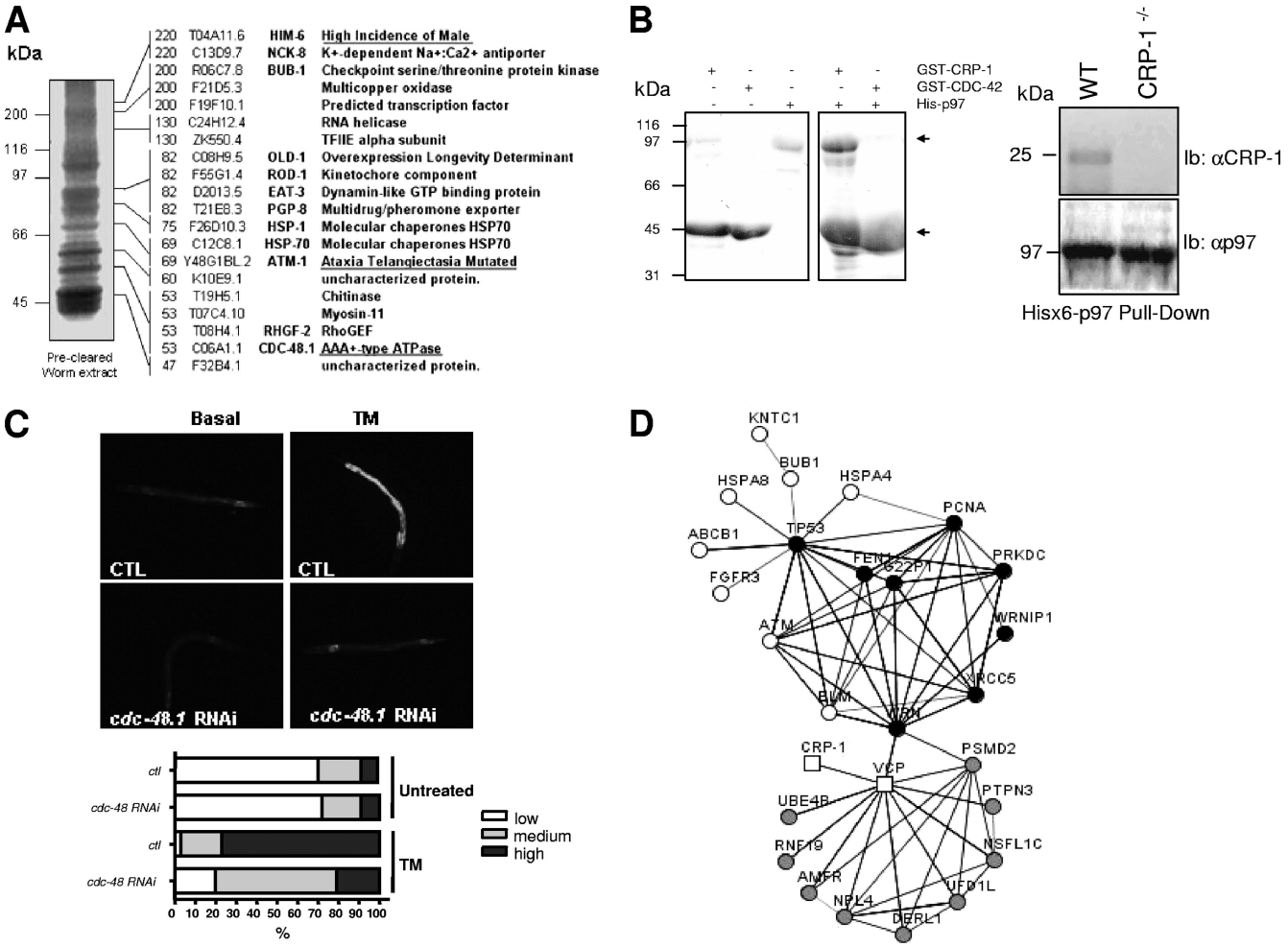

FIG. 4. CRP-1 interacts with a protein complex which includes CDC-48.1 and ATM-1. (A) SDS-PAGE of the GST–CRP-1 pull-down performed on precleared worm lysate, followed by mass spectrometry analysis (right). Peptides identified were annotated using the WormBase (http://www.wormbase.org/) sequence name as well as the *Caenorhabditis* Genetic Center (http://www.cbs.umn.edu/CGC/) three-letter name. (B, left) GST pull-down using GST–CRP-1 or GST–CDC-42 and mouse His_6-p97/VCP/CDC-48 recombinant proteins expressed in bacteria and resolved on SDS-PAGE gel stained with Coomassie blue R250. (Right) His_6-p97/VCP/CDC-48 pull-down was performed on wild-type (WT) (N2) or *crp-1*$^{-/-}$ total worm extract followed by immunoblot analysis using anti (α)-CRP-1 antibodies (HyperOmics Farma, Inc.) or anti-p97 antibodies. (C) Transcriptional regulation of *pckb-2*::*gfp* reporter by *cdc-48*. *pckb-2*::*gfp* transgenic worms were subjected or not to *cdc-48.1* RNAi as described in Materials and Methods. Following exposure to TM, *pckb-2*::*gfp* activation was visualized and quantified using fluorescence microscopy. (D) STRING network representation of the known and predicted interactions between proteins identified by mass spectrometry (white), VCP (p97/VCP/CDC-48) first-interacting proteins (gray), and ATM-1 first-interacting proteins (black). The edges are representative of the various interaction types available through STRING. Circles and squares are indicative of human and *C. elegans* genes, respectively (see also Table S3 in the supplemental material).

ternary complex comprising CRP-1, HIM-6, and CDC-48, with the last bridging the two others (Fig. 5C). This allowed us to build an interaction model where CRP-1 is in complex with HIM-6 through interaction with CDC-48. In this model, ATM-1 could play a regulatory role by phosphorylating both CDC-48 and HIM-6 since the mammalian orthologs of these proteins are established ATM substrates (26).

***C. elegans* resistance to ER stress is controlled though genetic interactions between *crp-1*, *cdc-48.1*, and *atm-1*.** To evaluate the functional relevance of such a complex, we hypothesized that CRP-1, CDC-48.1, and ATM-1 could constitute a functional protein complex involved in an ER stress-mediated transcriptional regulatory pathway. We then postulated that mutations in these proteins would cause defects in their ER stress-adaptive capacity. Consequently, we tested the susceptibility of wild-type and knockout strains subjected to treatments with increasing TM concentrations. Under basal conditions, wild-type worms (N2) as well as *crp-1* (*ok685*), *cdc-48.1* (*tm544*), and *atm-1* (*gk186*) knockout strains developed normally and the growth rate of wild-type (N2) worms was not affected until the concentration of TM reached 5 μg/ml (Fig. 6A and B). At this concentration, less than 20% of the N2 worms failed to develop to adults. In contrast, *crp-1*$^{-/-}$, *atm-1*$^{-/-}$, and to a lesser extent *cdc-48*.1$^{-/-}$ knockout strains were more sensitive to TM than N2 worms (Fig. 6A and B). At 2 μg/ml of TM, more than 60% of all the *crp-1*$^{-/-}$ mutants and 30% of the *atm-1*$^{-/-}$ mutants were arrested at the L1 larval stages compared to less than 1% of wild-type worms. *Cdc-*

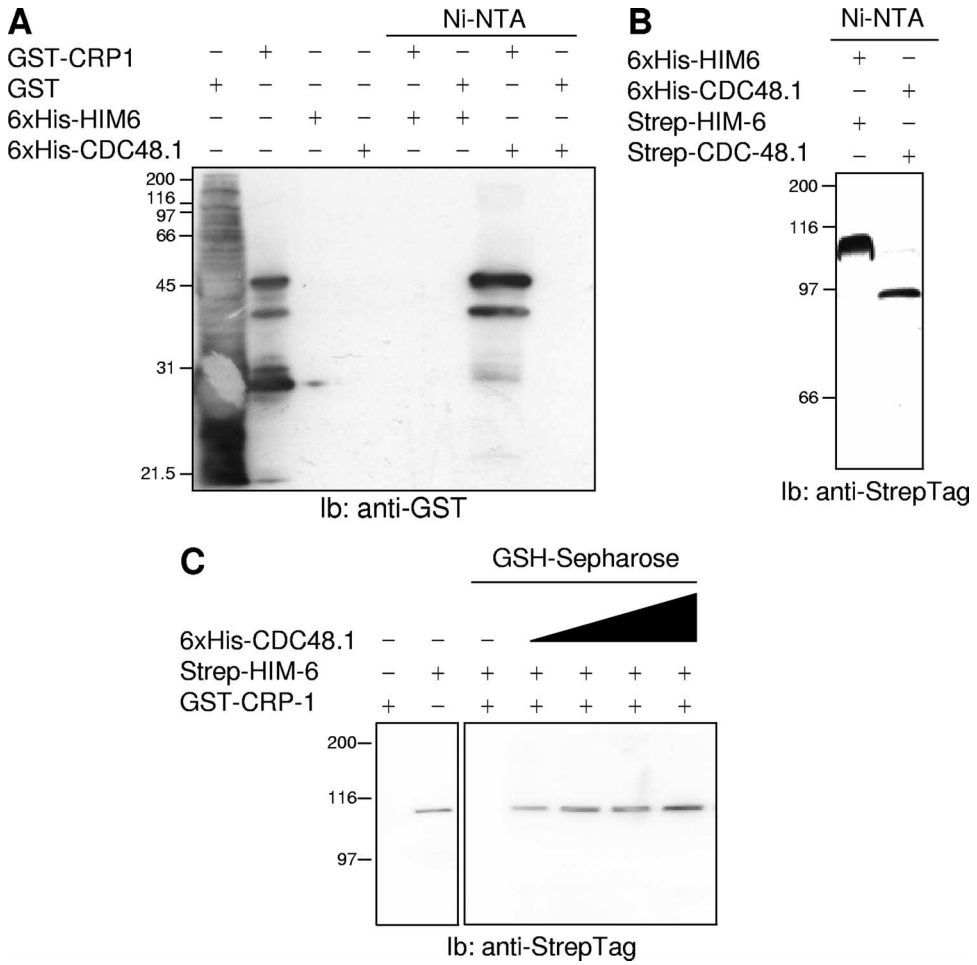

FIG. 5. Physical interactions between CRP-1, HIM-6, and CDC-48. (A) Binary interactions between CRP-1 and either His_6–HIM-6 or His_6–CDC-48. The purified proteins were pulled-down using Ni-NTA-agarose beads, and the presence of GST–CRP-1 was revealed by immunoblotting (Ib) using anti-GST antibodies. (B) Binary interactions between His_6–CDC-48.1 and Strep-tagged HIM-6 or His_6–HIM-6 and Strep-tagged CDC-48.1 following purification of the complex by Ni-NTA-agarose beads and analysis by immunoblotting using anti-Strep tag antibodies. (C) Ternary complex including CRP-1, HIM-6, and CDC-48.1. Increasing concentrations of His_6–CDC-48.1 were added to an equimolar mixture of GST–CRP-1 and Strep-tagged HIM-6. Following 1 h of incubation on ice, the complex was pulled-down using glutathione-Sepharose beads and the presence of HIM-6 in the complex was evaluated by immunoblotting using anti-Strep tag antibodies.

48.1$^{-/-}$ mutants displayed a similar phenotype at a 5-μg/ml concentration of TM, where 70% of *cdc-48.1*$^{-/-}$ mutants failed to develop to adults compared to 20% of wild-type animals. These results suggest that *crp-1*, *cdc-48.1*, and *atm-1* are required for worm adaptation to stress conditions and for larva development.

To further investigate this observation, we aimed at establishing functional interactions between these three genes. Identification of genetic interactions is a useful way to investigate functional relationships between two genes. Consequently, we subjected *atm-1*$^{-/-}$ and *cdc-48.1*$^{-/-}$ knockout strains to RNAi treatment targeting *crp-1* and measured the resistance of these double mutants to TM. Interestingly, in both conditions, reduction of *crp-1* expression suppressed the hypersensitivity of *cdc-48*$^{-/-}$ and *atm-1*$^{-/-}$ mutants to TM (Fig. 6C). Indeed, when sujected to 5 μg/ml *crp-1* RNAi, a *cdc-48.1*$^{-/-}$ mutant exhibited development rates similar to that of N2 worms, with 80% of the animals developing normally. In a similar manner, exposure to 2-μg/ml *crp-1* silencing of an *atm-1*$^{-/-}$ mutant led to better resistance to TM and 90% of the animals were able to develop to adult stages. An attenuating phenotype was also observed when the *atm-1*$^{-/-}$ strain was subjected to *cdc-48.1* RNAi (Fig. 6D). These results show that *crp-1*, *atm-1*, and *cdc-48* interact genetically and may then have antagonistic functions with respect to an ER stress signaling event occurring upon TM treatment. In addition, these results led us propose the existence of an alternative, ERAD-independent p97/VCP/CDC-48 pathway. Indeed, this protein may associate with a functional complex containing CRP-1 and ATM-1 to regulate the transcriptional level of UPR-induced genes (Fig. 6) in a manner similar to that occurring in the IRE-1/XBP-1 axis (see Fig. S2 in the supplemental material).

Genetic interactions between CRP-1 and the UPR components. In an attempt to further dissect the role of CRP-1 in the ER stress response, we analyzed using RT-PCR the expression of seven genes, *hsp-4*, *srp-7*, *dnj-27*, *cht-1*, *ckb-2*, *F22E5.6*, and *xbp-1*, that were previously reported to be specifically regulated by the UPR (42, 45). These genes were selected on the basis of

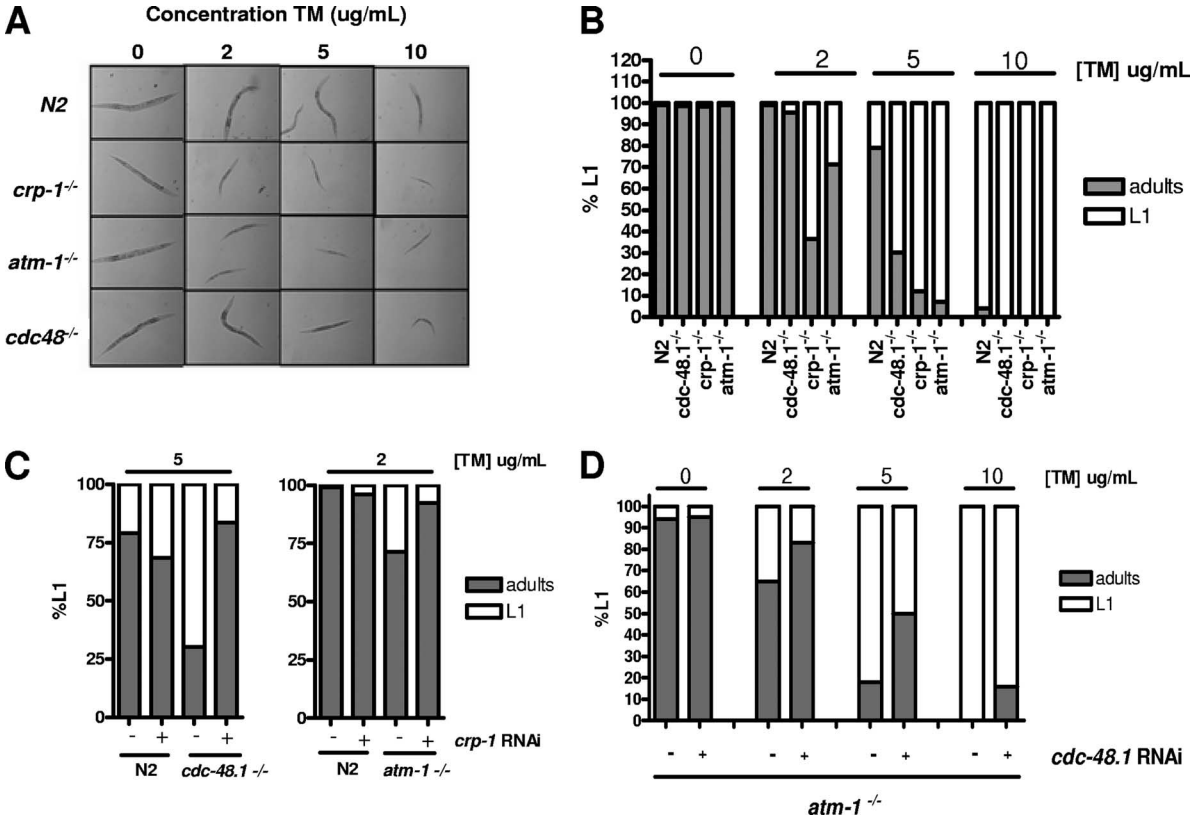

FIG. 6. *crp-1*$^{-/-}$, *atm-1*$^{-/-}$, and *cdc-48.1*$^{-/-}$ mutants are hypersensitive to TM and interact genetically. (A) Pictures showing the average sizes of wild-type (N2) and mutant worms when exposed to different concentrations of TM. (B) The percentage of progeny arrested in the L1 stage of development was plotted against the different concentrations of TM for the wild-type worms (N2) and *cdc-48.1*$^{-/-}$ (tm544), *crp-1*$^{-/-}$ (ok685), and *atm-1*$^{-/-}$ (gk186) mutants. (C and D) The percentage of progeny arrested in L1 stages of development was plotted against the different concentrations of TM for *cdc-48.1*$^{-/-}$ and *atm-1*$^{-/-}$ mutants subjected of not to *crp-1* RNAi (C) and for the *atm-1*$^{-/-}$ mutant subjected of not to *cdc-48* RNAi (D).

two transcriptome analyses (42, 45). The expression of the corresponding mRNAs was normalized using the expression levels of *ama-1*, previously reported not to be a UPR target (22). To evaluate the expression levels of the mRNAs, N2 or *crp-1*$^{-/-}$ worms were treated with TM, DTT (oxidative stress), or sodium azide (hypoxia) as described in Materials and Methods. Interestingly, the absence of CRP-1 did not significantly affect the expression levels of *srp-7*. More importantly, a differential response was observed for the other genes, with attenuated expression in *crp-1*$^{-/-}$ worms of *xbp-1* and *ckb-2* and increased expression of *hsp-4* and *F22E5.6* (Fig. 7 A and B). The response also varied depending on the stress applied to the worms, as observed in Fig. 2. In addition, we assessed the effect on the splicing of *xbp-1* mRNA of the above-mentioned stresses. mRNA splicing was slightly attenuated upon TM treatment in *crp-1*$^{-/-}$ animals but remained unchanged upon treatment with other stressors (Fig. 7C; $P < 0.02$).

As the above-selected genes were found to be downstream of PEK-1/IRE1 (*F22E5.6*), ATF-6/IRE-1 (*cht-1*, *xbp-1*), or IRE1 (*srp-7*, *dnj-27*, *hsp-4*, *ckb-2*) signaling, our next objective was to evaluate the genetic interactions between *crp-1* and the three proximal ER stress sensors, PEK-1, ATF-6, and IRE-1. To this end, *pek-1*$^{-/-}$ and *atf-6*$^{-/-}$ worms were subjected to *crp-1* RNAi and treated or not with increasing concentrations of TM (2 or 5 μg/ml). To evaluate the genetic interaction between *crp-1* and *ire-1*, the opposite experiment was performed: we used *crp-1*$^{-/-}$ animals and subjected them to *xbp-1* RNAi. This experiment was carried out since the *ire-1*$^{-/-}$ strain showed a developmental defect in the early stage and was very sensitive to TM. Interestingly, *crp-1* silencing did not significantly affect the sensitivity of *pek-1*$^{-/-}$ animals to TM (Fig. 8A and B). In contrast, when *crp-1* was silenced in *atf-6*$^{-/-}$ animals, the worms turned out to be less sensitive to TM treatment than nonsilenced animals, thus suggesting that CRP-1 may function synergistically with ATF-6 to transduce adaptive signals (Fig. 8C). Interestingly, this phenomenon correlates with the observed up-regulation of total *xbp-1* mRNA in *crp-1*$^{-/-}$ animals upon TM treatment, as *xbp-1* was previously described as a transcriptional target of ATF-6.

DISCUSSION

ER stress is a physiological response that occurs in normal processes such as plasma cell differentiation (31), insulin secretion by pancreatic beta cells (14), and cytokinesis (3). In addition, it can be activated in the course of environmental perturbation and diseases (14, 29, 31). Although the molecular entities and mechanisms involved in the activation and trans-

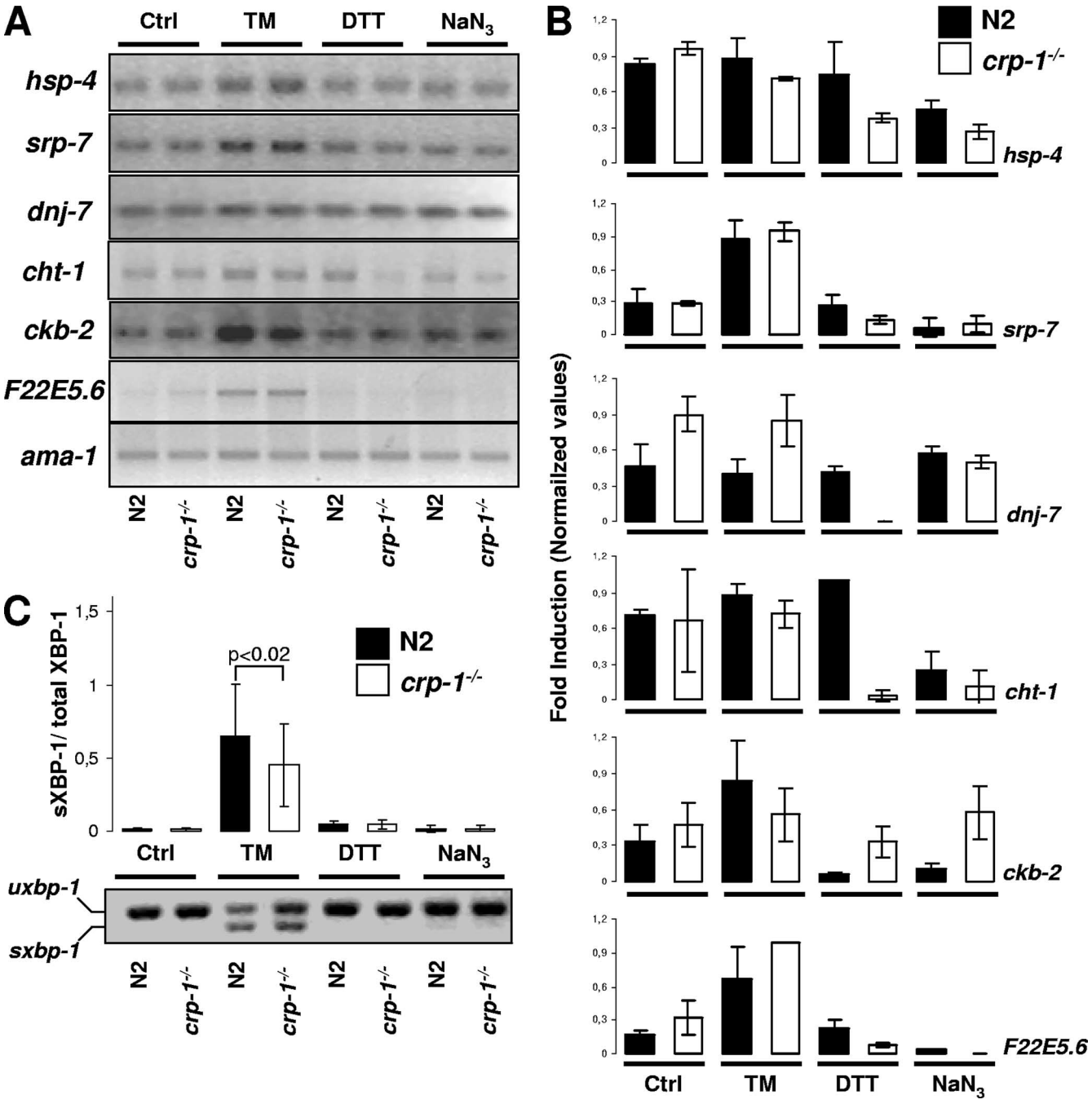

FIG. 7. CRP-1-dependent regulation of the UPR transcriptional response. (A) Evaluation of the expression of the UPR target genes *hsp-4*, *srp-7*, *dnj-7*, *cht-1*, *ckb-2*, and *F22E5.6* by RT-PCR analysis on mRNA isolated from worms treated or not with 5 μg/ml TM or 2 mM DTT for 5 h or 10 mM sodium azide for 90 min. PCR products are visualized following resolution by agarose gel electrophoresis, staining with ethidium bromide, and UV transillumination. Ctrl, control. (B) Quantification of the gels presented in panel A. Values relative to the expression of a control mRNA (*ama-1*) are reported and were obtained following normalization. The graphs represent the averages of three independent experiments ± standard deviations (SD). (C) Assessment of *xbp-1* mRNA splicing using RT-PCR on mRNA collected as described above. PCR products are visualized followed resolution by agarose gel electrophoresis, staining with ethidium bromide, and UV transillumination (bottom). The graph shows the quantification of spliced *xbp-1* mRNA (sXBP-1)/spliced plus unspliced *xbp-1* mRNA (total XBP-1) as deduced from three independent experiments ± SD.

mission of ER stress signals have been really well characterized in the past 10 years (30, 38, 41), the existence of regulatory pathways remains to be investigated.

In an attempt to identify novel regulators of the UPR, we characterized eight GFP reporters to allow rapid and efficient detection of ER stress in living *C. elegans*. Only two reporters, *pF48E3.3*::*gfp* and *pbre-1*::*gfp*, were not responsive to TM. Besides a per se nonresponsiveness to ER stress, the lack of

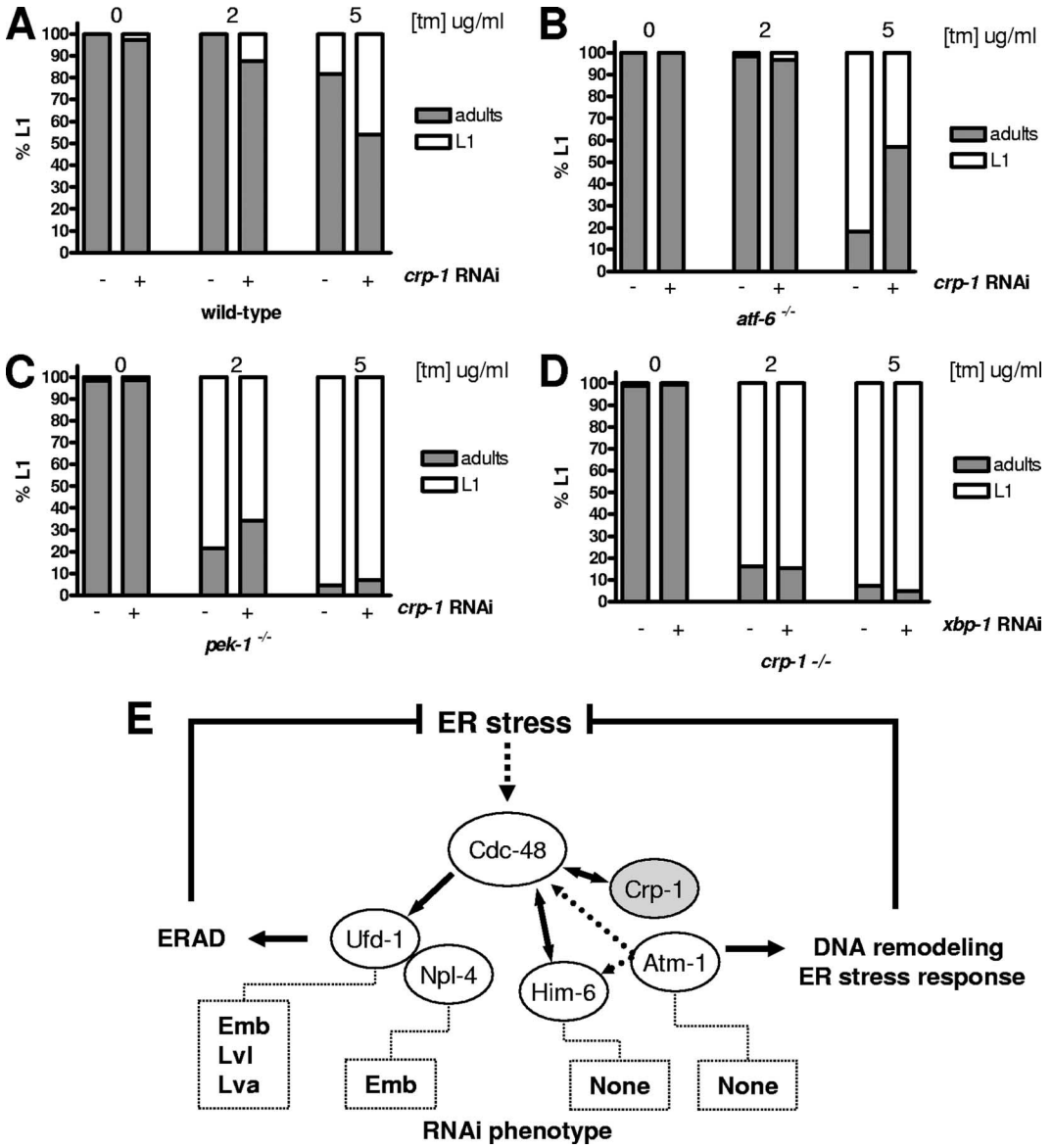

FIG. 8. Genetic interaction map linking *crp-1* and the UPR proximal sensors. (A to C) The percentage of progeny arrested in the L1 stage of development was plotted against different concentrations of TM (2 or 5 μg/ml) for N2 (A), *pek-1*$^{-/-}$ (B), and *atf-6*$^{-/-}$ (C) animals subjected or not to *crp-1* RNAi. (D) The percentage of progeny arrested in the L1 stage of development was plotted against different concentrations of TM (2 or 5 μg/ml) for *crp-1*$^{-/-}$ animals subjected to *xbp-1* RNAi. (E) Schematic representation of CDC-48-dependent pathways proposed to explain the implication of CRP-1, HIM-6, and ATM-1 in the regulation of ER homeostasis during stress condition through DNA remodeling/transcriptional processes.

induction of these two reporters could be attributed to (i) gene expression exclusively in tissues or cells that are less exposed to TM, (ii) fluorescence levels too low to be detected using the Copas Biosort, or finally (iii) the region cloned to construct the GFP reporter not including all the regulatory elements required for promoter activation. We selected three specific reporters that were highly induced upon ER stress and displayed major intestinal expression. Interestingly, the activation of the different reporter construct-selected promoters was dependent on the ER stress inducer (TM, AZC, DTT, or TG) used for our experiment, supporting the conservation in *C. elegans* of a UPR machinery known to be extremely complex and multimodular in mammals (42). To provide functional insights into regulatory mechanisms taking place during UPR activation, we used a reverse genetic approach combining gene silencing and analysis of in vivo GFP reporters upon basal and ER stress conditions. At first, we evaluated the role of 13 GTPases either localized in the ER or along the secretory pathway or implicated in ER-related function to increase the chances of affecting ER stress signaling. The silencing of most of the GTPases did not show any effect on the reporter. Even if the entire reading frames were used to perform the RNAi, we could not exclude the possibility that these negative observations may result from RNAi inefficiency in degrading target mRNAs.

Indeed, many factors can dramatically reduce the effectiveness of an RNAi experiment. First, dsRNA introduced into the worms might not be abundant enough to completely degrade the target mRNA. This is particularly true for mRNAs that are highly expressed or which have a low turnover (long half-life). The tissue localization of the GTPase mRNA is also an important factor to consider. Since the GFP reporter used in our experiments was mainly expressed in the worm intestine, GTPases expressed in other tissues might have a lower impact on the activation of this promoter.

Our experimental approach allowed us to identify three GTPases, namely, SAR-1, CDC-42, and CRP-1, as important regulators of ER stress signaling under either basal or stress conditions. Indeed silencing of SAR-1, which belongs to the COPII complex, led to the activation of ER stress under basal conditions. This observation could be explained by the required presence of SAR-1 for protein progression from the ER; the resulting protein accumulation may be sufficient to saturate ER folding capacity and lead to ER stress.

On the other hand, silencing of CDC-42 and CRP-1 prevented TM-induced *pckb-2*::*gfp* activation. These proteins are two homologous member of the Rho subfamily of GTPases. We then sought to investigate the molecular mechanisms responsible for this observation. To this end, CRP-1-interacting partners were characterized by CRP-1–GST pull-down followed by mass spectrometry analysis. Integration of these data to a STRING-based (46, 47) functional network representation of CRP-1 partners showed that most of the hits identified were involved in transcriptional and DNA-monitoring/repair processes. We showed that the transcription-regulatory role of CRP-1 also required a direct interaction with the AAA^+ ATPase CDC-48.1. It is noteworthy that both genetic and physical interactions between GTPases of the RAS superfamily and AAA ATPases have been reported in the literature to be relevant to specific physiological and pathological mechanisms (12, 44).

CDC-48 is a mostly cytosolic chaperone involved in several cellular pathways, such as organelle maintenance through homotypic membrane fusion of the ER, Golgi apparatus, and nuclear envelope, and degradation of misfolded proteins via ERAD (13). This protein is homologous to the mammalian P97/VCP/CDC-48, which is also found in the nucleus and directly binds to the RecQ domain of Werner syndrome helicase (WRN) (18, 32). Interestingly, when we characterized CRP-1-interacting proteins, we found the *C. elegans* Bloom syndrome helicase homolog HIM-6, which shows a RecQ domain conserved with that of WRN. Moreover, in the complex, we also detected the ATM-1 kinase, which is known to phosphorylate BLM and VCP in mammalian systems (26). We confirmed that CRP-1 can directly interact with CDC-48 in vitro but not with HIM-6. The CRP-1/HIM-6 complex was made possible by the presence of CDC-48, which bridges those proteins (Fig. 5). The role of ATM-1 in this complex remains to be further investigated. However, as BLM (the HIM-6 mammalian ortholog) and P97/VCP (the CDC-48 mammalian ortholog) are both ATM substrates, this kinase may represent a key regulatory component of the DNA remodeling/transcriptional functions of the complex. As a consequence, we believe that CDC-48 might act as a scaffold to create a new functional complex between HIM-6, CRP-1, and possibly ATM-1, which could in turn activate/inactivate specific transcriptional programs, as evidenced in Fig. 7A and B.

In addition, we propose a novel role for P97/VCP/CDC-48 in the regulation of ER stress. Indeed, this protein could function in parallel (and perhaps independently) to ERAD because (i) none of the CRP-1-interacting partners found in the P97/VCP/CDC-48 functional subnetwork were implicated in ERAD and membrane fusion (Fig. 5D), (ii) these two events are known to occur in different subcellular compartments, with ERAD occurring mainly in the cytosol, whereas the mechanisms identified here are believed to take place in the nucleus, and finally (iii) silencing of P97/VCP/CDC-48-interacting partners involved in ERAD (NPL-4 and UFD-1) leads to lethal phenotypes, which is not the case for HIM-6 and ATM-1 (Fig. 6). The last observation may rely on the fact that either the CDC-48-dependent transcriptional program activated in response to ER stress is dispensable or redundant mechanisms can compensate for the absence of HIM-6 (e.g., WRN-1) or ATM-1 (e.g., ATL-1).

In addition to this evidence, we have demonstrated that *crp-1* genetically interacted with *atf-6*, as the absence of CRP-1 decreased the sensitivity of ATF-6-deficient but not PEK-1-deficient worms to TM (Fig. 8). This suggested that, similar what that occurs in the IRE-1/XBP-1 axis (see Fig. S2 in the supplemental material), the CRP-1/CDC-48/HIM-6 complex is implicated in the regulation of subsets of genes required for ER stress adaptation. This phenomenon could potentially be explained by the substantial redistribution of CRP-1 from punctate structures to more-diffuse areas, which is observed upon TM treatment (see Fig. S3 in the supplemental material). Although the subcellular localization of the complex and its dynamics remain to be fully investigated, our data suggest that TM treatment may alter the localization of CRP-1 and CDC-48 to promote their nuclear localization (see Fig. S3 in the supplemental material) (32) by a yet-undetermined mechanism. In this compartment, a ternary complex between CRP-1, CDC-48, and HIM-6 may form to promote DNA remodeling/gene transcription control. This complex may then be regulated by the activation of the ATM-1 pathway (stabilized or destabilized), as suggested by the observation, made by Partridge and colleagues, that in mammalian cells DNA damage, an ATM activator, promotes the dissociation of the RecQ helicase WRN from the CDC-48 ortholog P97/VCP (32).

Our results unravel the existence of a novel pathway dependent on the GTP binding protein CRP-1 and the AAA+ ATPase CDC-48 which controls a specific UPR-mediated transcriptional response to promote cell adaptation to ER stress. This pathway may be dependent on DNA remodeling mechanisms, as indicated by the complex formed by CRP-1, CDC-48, and the RecQ DNA helicase HIM-6, and may be activated independently of ERAD (Fig. 8E).

ACKNOWLEDGMENTS

We thank A. Higa-Nishiyama for help with confocal microscopy and O. Pluquet, V. Moreau, M. Dominguez, and P. Legembre for critical reading of the manuscript. We also thank the *Caenorhabditis* Genetics Center for *C. elegans* strains.

This work was supported by grants from the Fond de Recherche en Santé du Québec, INSERM (Avenir), and a Marie Curie reintegration grant to E.C. M.E.C. was a recipient of a FRNTQ Ph.D. studentship.

REFERENCES

1. **Ababou, M., S. Dutertre, Y. Lecluse, R. Onclercq, B. Chatton, and M. Amor-Gueret.** 2000. ATM-dependent phosphorylation and accumulation of endogenous BLM protein in response to ionizing radiation. Oncogene **19:** 5955–5963.
2. **Altan-Bonnet, N., R. Sougrat, and J. Lippincott-Schwartz.** 2004. Molecular basis for Golgi maintenance and biogenesis. Curr. Opin. Cell Biol. **16:**364–372.
3. **Bicknell, A. A., A. Babour, C. M. Federovitch, and M. Niwa.** 2007. A novel role in cytokinesis reveals a housekeeping function for the unfolded protein response. J. Cell Biol. **177:**1017–1027.
4. **Braakman, I., J. Helenius, and A. Helenius.** 1992. Manipulating disulfide bond formation and protein folding in the endoplasmic reticulum. EMBO J. **11:**1717–1722.
5. **Brenner, S.** 1974. The genetics of *Caenorhabditis elegans*. Genetics **77:**71–94.
6. **Calfon, M., H. Zeng, F. Urano, J. H. Till, S. R. Hubbard, H. P. Harding, S. G. Clark, and D. Ron.** 2002. IRE1 couples endoplasmic reticulum load to secretory capacity by processing the XBP-1 mRNA. Nature **415:**92–96.
7. **Caruso, M. E., and E. Chevet.** 2007. Systems biology of the endoplasmic reticulum stress response. Subcell. Biochem. **43:**277–298.
8. **Caruso, M. E., S. Jenna, S. Beaulne, E. H. Lee, A. Bergeron, C. Chauve, P. Roby, J. F. Rual, D. E. Hill, M. Vidal, R. Bosse, and E. Chevet.** 2005. Biochemical clustering of monomeric GTPases of the Ras superfamily. Mol. Cell. Proteomics **4:**936–944.
9. **Chevet, E., P. H. Cameron, M. F. Pelletier, D. Y. Thomas, and J. J. Bergeron.** 2001. The endoplasmic reticulum: integration of protein folding, quality control, signaling and degradation. Curr. Opin. Struct. Biol. **11:**120–124.
10. **Chevet, E., C. A. Jakob, D. Y. Thomas, and J. J. Bergeron.** 1999. Calnexin family members as modulators of genetic diseases. Semin. Cell Dev. Biol. **10:**473–480.
11. **Dupuy, D., N. Bertin, C. A. Hidalgo, K. Venkatesan, D. Tu, D. Lee, J. Rosenberg, N. Svrzikapa, A. Blanc, A. Carnec, A. R. Carvunis, R. Pulak, J. Shingles, J. Reece-Hoyes, R. Hunt-Newbury, R. Viveiros, W. A. Mohler, M. Tasan, F. P. Roth, C. Le Peuch, I. A. Hope, R. Johnsen, D. G. Moerman, A. L. Barabasi, D. Baillie, and M. Vidal.** 2007. Genome-scale analysis of in vivo spatiotemporal promoter activity in *Caenorhabditis elegans*. Nat. Biotechnol. **25:**663–668.
12. **Evans, K., C. Keller, K. Pavur, K. Glasgow, B. Conn, and B. Lauring.** 2006. Interaction of two hereditary spastic paraplegia gene products, spastin and atlastin, suggests a common pathway for axonal maintenance. Proc. Natl. Acad. Sci. USA **103:**10666–10671.
13. **Halawani, D., and M. Latterich.** 2006. p97: the cell's molecular purgatory? Mol. Cell **22:**713–717.
14. **Harding, H. P., and D. Ron.** 2002. Endoplasmic reticulum stress and the development of diabetes: a review. Diabetes **51**(Suppl. 3)**:**S455–S461.
15. **Hemming, F. W.** 1982. Control and manipulation of the phosphodolichol pathway of protein N-glycosylation. Biosci. Rep. **2:**203–221.
16. **Hooper, S. D., and P. Bork.** 2005. Medusa: a simple tool for interaction graph analysis. Bioinformatics **21:**4432–4433.
17. **Hunt-Newbury, R., R. Viveiros, R. Johnsen, A. Mah, D. Anastas, L. Fang, E. Halfnight, D. Lee, J. Lin, A. Lorch, S. McKay, H. M. Okada, J. Pan, A. K. Schulz, D. Tu, K. Wong, Z. Zhao, A. Alexeyenko, T. Burglin, E. Sonnhammer, R. Schnabel, S. J. Jones, M. A. Marra, D. L. Baillie, and D. G. Moerman.** 2007. High-throughput in vivo analysis of gene expression in *Caenorhabditis elegans*. PLoS Biol. **5:**e237.
18. **Indig, F. E., J. J. Partridge, C. von Kobbe, M. I. Aladjem, M. Latterich, and V. A. Bohr.** 2004. Werner syndrome protein directly binds to the AAA ATPase p97/VCP in an ATP-dependent fashion. J. Struct. Biol. **146:**251–259.
19. **Jenna, S., M. E. Caruso, A. Emadali, D. T. Nguyen, M. Dominguez, S. Li, R. Roy, J. Reboul, M. Vidal, G. N. Tzimas, R. Bosse, and E. Chevet.** 2005. Regulation of membrane trafficking by a novel Cdc42-related protein in *Caenorhabditis elegans* epithelial cells. Mol. Biol. Cell **16:**1629–1639.
20. **Jenna, S., and E. Chevet.** 2007. High-throughput RNAi in *Caenorhabditis elegans*—from molecular phenotypes to pathway analysis, p. 158. *In* M. Latterich (ed.), RNAi. Taylor and Francis, New York, NY.
21. **Kamath, R. S., A. G. Fraser, Y. Dong, G. Poulin, R. Durbin, M. Gotta, A. Kanapin, N. Le Bot, S. Moreno, M. Sohrmann, D. P. Welchman, P. Zipperlen, and J. Ahringer.** 2003. Systematic functional analysis of the *Caenorhabditis elegans* genome using RNAi. Nature **421:**231–237.
22. **Kapulkin, W. J., B. G. Hiester, and C. D. Link.** 2005. Compensatory regulation among ER chaperones in *C. elegans*. FEBS Lett. **579:**3063–3068.
23. **Lavoie, C., E. Chevet, L. Roy, N. K. Tonks, A. Fazel, B. I. Posner, J. Paiement, and J. J. Bergeron.** 2000. Tyrosine phosphorylation of p97 regulates transitional endoplasmic reticulum assembly in vitro. Proc. Natl. Acad. Sci. USA **97:**13637–13642.
24. **Lazarow, P. B.** 2003. Peroxisome biogenesis: advances and conundrums. Curr. Opin. Cell Biol. **15:**489–497.
25. **Luna, A., O. B. Matas, J. A. Martinez-Menarguez, E. Mato, J. M. Duran, J. Ballesta, M. Way, and G. Egea.** 2002. Regulation of protein transport from the Golgi complex to the endoplasmic reticulum by CDC42 and N-WASP. Mol. Biol. Cell **13:**866–879.
26. **Matsuoka, S., B. A. Ballif, A. Smogorzewska, E. R. McDonald III, K. E. Hurov, J. Luo, C. E. Bakalarski, Z. Zhao, N. Solimini, Y. Lerenthal, Y. Shiloh, S. P. Gygi, and S. J. Elledge.** 2007. ATM and ATR substrate analysis reveals extensive protein networks responsive to DNA damage. Science **316:**1160–1166.
27. **McKay, S. J., R. Johnsen, J. Khattra, J. Asano, D. L. Baillie, S. Chan, N. Dube, L. Fang, B. Goszczynski, E. Ha, E. Halfnight, R. Hollebakken, P. Huang, K. Hung, V. Jensen, S. J. Jones, H. Kai, D. Li, A. Mah, M. Marra, J. McGhee, R. Newbury, A. Pouzyrev, D. L. Riddle, E. Sonnhammer, H. Tian, D. Tu, J. R. Tyson, G. Vatcher, A. Warner, K. Wong, Z. Zhao, and D. G. Moerman.** 2003. Gene expression profiling of cells, tissues, and developmental stages of the nematode *C. elegans*. Cold Spring Harbor Symp. Quant. Biol. **68:**159–169.
28. **Memon, A. R.** 2004. The role of ADP-ribosylation factor and SAR1 in vesicular trafficking in plants. Biochim. Biophys. Acta **1664:**9–30.
29. **Moenner, M., O. Pluquet, M. Bouchecareilh, and E. Chevet.** 2007. Integrated endoplasmic reticulum stress responses in cancer. Cancer Res. **67:**10631–10634.
30. **Mori, K.** 2004. Unfolded protein response as a quality control mechanism of proteins. Tanpakushitsu Kakusan Koso **49:**992–997. (In Japanese.)
31. **Otsu, M., and R. Sitia.** 2007. Diseases originating from altered protein quality control in the endoplasmic reticulum. Curr. Med. Chem. **14:**1639–1652.
32. **Partridge, J. J., J. O. Lopreiato, Jr., M. Latterich, and F. E. Indig.** 2003. DNA damage modulates nucleolar interaction of the Werner protein with the AAA ATPase p97/VCP. Mol. Biol. Cell **14:**4221–4229.
33. **Philips, M. R.** 2005. Compartmentalized signalling of Ras. Biochem. Soc. Trans. **33:**657–661.
34. **Philips, M. R.** 2004. Sef: a MEK/ERK catcher on the Golgi. Mol. Cell **15:**168–169.
35. **Quatela, S. E., and M. R. Philips.** 2006. Ras signaling on the Golgi. Curr. Opin. Cell Biol. **18:**162–167.
36. **Rao, V. A., A. M. Fan, L. Meng, C. F. Doe, P. S. North, I. D. Hickson, and Y. Pommier.** 2005. Phosphorylation of BLM, dissociation from topoisomerase IIIα, and colocalization with γ-H2AX after topoisomerase I-induced replication damage. Mol. Cell. Biol. **25:**8925–8937.
37. **Reboul, J., P. Vaglio, J. F. Rual, P. Lamesch, M. Martinez, C. M. Armstrong, S. Li, L. Jacotot, N. Bertin, R. Janky, T. Moore, J. R. Hudson, Jr., J. L. Hartley, M. A. Brasch, J. Vandenhaute, S. Boulton, G. A. Endress, S. Jenna, E. Chevet, V. Papasotiropoulos, P. P. Tolias, J. Ptacek, M. Snyder, R. Huang, M. R. Chance, H. Lee, L. Doucette-Stamm, D. E. Hill, and M. Vidal.** 2003. *C. elegans* ORFeome version 1.1: experimental verification of the genome annotation and resource for proteome-scale protein expression. Nat. Genet. **34:**35–41.
38. **Ron, D., and P. Walter.** 2007. Signal integration in the endoplasmic reticulum unfolded protein response. Nat. Rev. Mol. Cell Biol. **8:**519–529.
39. **Sabala, P., M. Czarny, J. P. Woronczak, and J. Baranska.** 1993. Thapsigargin: potent inhibitor of Ca^{2+} transport ATP-ases of endoplasmic and sarcoplasmic reticulum. Acta Biochim. Pol. **40:**309–319.
40. **Saloheimo, M., H. Wang, M. Valkonen, T. Vasara, A. Huuskonen, M. Riikonen, T. Pakula, M. Ward, and M. Penttila.** 2004. Characterization of secretory genes *ypt1*/*yptA* and *nsf1*/*nsfA* from two filamentous fungi: induction of secretory pathway genes of *Trichoderma reesei* under secretion stress conditions. Appl. Environ Microbiol. **70:**459–467.
41. **Schroder, M., and R. J. Kaufman.** 2005. The mammalian unfolded protein response. Annu. Rev. Biochem. **74:**739–789.
42. **Shen, X., R. E. Ellis, K. Sakaki, and R. J. Kaufman.** 2005. Genetic interactions due to constitutive and inducible gene regulation mediated by the unfolded protein response in *C. elegans*. PLoS Genet. **1:**e37.
43. **Takeuchi, M., T. Ueda, K. Sato, H. Abe, T. Nagata, and A. Nakano.** 2000. A dominant negative mutant of sar1 GTPase inhibits protein transport from the endoplasmic reticulum to the Golgi apparatus in tobacco and *Arabidopsis* cultured cells. Plant J. **23:**517–525.
44. **Tanaka, H., H. Fujita, H. Katoh, K. Mori, and M. Negishi.** 2002. Vps4-A (vacuolar protein sorting 4-A) is a binding partner for a novel Rho family GTPase, Rnd2. Biochem. J. **365:**349–353.
45. **Urano, F., M. Calfon, T. Yoneda, C. Yun, M. Kiraly, S. G. Clark, and D. Ron.** 2002. A survival pathway for *Caenorhabditis elegans* with a blocked unfolded protein response. J. Cell Biol. **158:**639–646.
46. **von Mering, C., M. Huynen, D. Jaeggi, S. Schmidt, P. Bork, and B. Snel.** 2003. STRING: a database of predicted functional associations between proteins. Nucleic Acids Res. **31:**258–261.
47. **von Mering, C., L. J. Jensen, M. Kuhn, S. Chaffron, T. Doerks, B. Kruger, B. Snel, and P. Bork.** 2007. STRING 7–recent developments in the integration and prediction of protein interactions. Nucleic Acids Res. **35:**D358–D362.
48. **Wojcik, C., M. Rowicka, A. Kudlicki, D. Nowis, E. McConnell, M. Kujawa, and G. N. DeMartino.** 2006. Valosin-containing protein (p97) is a regulator of endoplasmic reticulum stress and of the degradation of N-end rule and ubiquitin-fusion degradation pathway substrates in mammalian cells. Mol. Biol. Cell **17:**4606–4618.